Characteristics of MOR-Framework Zeolites Synthesized in Fluoride-Containing Media and Related Ordered Distribution of Al Atoms in the Framework

Masanao Kato,[†,§] Keiji Itabashi,[‡] Akihiko Matsumoto,*[,†] and Kazuo Tsutsumi[†]

Center for Chemometrics and School of Materials Science, Toyohashi University of Technology, Tempaku-cho, Toyohashi 441-8580, Japan, and Nanyo Research Laboratory, Tosoh Corporation, Shinnanyo 746-8501, Japan

Received: October 15, 2002; In Final Form: December 17, 2002

MOR type zeolites with Si/Al ratios of 5.19−9.00 have been synthesized in the presence of fluoride ion (denoted by MS-F). Although MS-F has the same framework topology as conventionally synthesized mordenite (MS-C), the characteristics of MS-F, such as crystal morphology, adsorptivity for benzene and thermal stability, are quite different from MS-C. Solid-state ^{29}Si MAS NMR measurements revealed that the number of Si atoms with a Si(2Al) environment in MS-F is less than that in MS-C of the same Si/Al ratio. Based upon the results of NMR measurements and those of benzene sorption and thermal stability, the ordered distribution of Al atoms in the framework of MS-F was determined by using the connectivity-configuration matrixes method under the restriction of Loewenstein's rule and the 2Al/5-ring avoidance rule. It is suggested that Al atoms are located at T_1, T_2, and T_4 sites in MS-F, which is different from the case of MS-C occupying T_1, T_2, T_3, and T_4 sites. The differences in the characteristics between MS-F and MS-C can be explained by the different distribution of Al atoms in their framework.

1. Introduction

Aluminosilicate zeolites have been widely used as adsorbents, catalysts, and ion exchangers.[1] Because of the value in utilization, the preparation and application of novel zeolites have been extensively studied.[2−4] Specific zeolitic properties, such as molecular adsorptivity, acidity, and molecular diffusivity, arise from aluminum ions in the zeolite framework accompanied by extraframework protons and/or metal cations. Therefore, the distribution of the Al ions over the available sites in the zeolitic framework has a large effect on the characteristics of a zeolite. Takaishi et al.[5] have proposed a novel method, the connectivity-configuration matrixes (CCM) method, to determine the Al atom distribution across possible sites and a new rule, the 2Al/5-ring avoidance rule, which complements Loewenstein's rule. The 2Al/5-ring avoidance rule states that no more than one Al atom can be located in a 5-ring.[5] It can be regarded as a specific manifestation of Dempsey rule. The applicability of the CCM method and the validity of the 2Al/5-ring avoidance rule have been examined for some zeolites containing 5-rings in their framework, i.e., mordenite, ferrierite,[5] epistilbite,[6] heulandite-clinoptilolite,[7] and dachiardite,[8] and it is found that this rule is satisfied in the synthetic and natural zeolites including monovalent cations as an extraframework species except for bikitite.[8] Especially, in the case of heulandite and clinoptilolite, the ordered distributions of Al atoms are different between these zeolites despite their identical framework topology. The differences in their Al configuration have been involved to explain their differing thermal stabilities.[7]

MOR-framework zeolites with Si/Al ratios of 5.10−9.55, which have been hydrothermally synthesized in alkaline media (denoted by MS-C),[9] can be synthesized in a fluoride-containing media (MS-F)[10,11] as can be other zeolites, MFI,[10,12] FER,[10,13] and *BEA.[10,14] The characteristics of MS-F, such as hydrothermal stability and molecular adsorptivity, are different from those of MS-C even though their Al content is identical.[15,16] The different properties might be expected to originate from different distributions of Al atoms within their frameworks as observed for heulandite and clinoptilolite.[7]

In the present study, MS-F of different Si/Al ratios were initially synthesized by literature procedures without adding seed crystals.[10,11] Then, the physicochemical properties of the prepared crystals were characterized and compared with those of MS-C. An ordered distribution of Al atoms in the framework of MS-F was elucidated by the CCM method.

2. Experimental Section

2.1. Synthesis. The chemical composition of reactant mixtures for the synthesis of MS-F is expressed as aNaF·3NaOH·$AlCl_3$·$b$$SiO_2$·$c$$H_2O$.[10,11] The values of a and b were controlled to obtain MS-F crystals with different Si/Al ratios as listed in Table 1. The value of the c/b ratio was kept constant at 30, and the total amount of a reactant mixture was kept at 50 g in all syntheses. The preparation procedure was as follows. Aluminum chloride ($AlCl_3$·$6H_2O$, 98%, Kanto Chemical) was dissolved in deionized water, and NaOH (99%, Tosoh Corp.) was added to precipitate aluminum hydroxides. While agitating the precipitate, NaF (98%, Kishida Chemical) was added to the suspension, and amorphous silica produced by a wet process (Nipsil VN-3, Nippon Silica Industrial Co., Ltd.) was then added to the suspension. After stirring the reactant mixture with a spatula for ca. 10 min, the mixture was transferred into a stainless steel autoclave with a volume of 80 mL and heated at 438−453 K for 72 h under an autogenous pressure while rotating at 50 rpm. After the hydrothermal treatment, the crystallized material was filtered and washed with hot water until the concentration of fluoride ion in the filtrate was less than 2×10^{-6} g/L.

* To whom correspondence should be addressed. Phone: +81-53-44-6911. Fax: +81-532-48-5833. E-mail: aki@tutms.tut.ac.jp.
† Toyohashi University of Technology.
‡ Tosoh Corporation.
§ Present address: Nagaoka National College of Technology, 888 Nishikatagai, Nagaoka 940-8532, Japan. E-mail: mkato@nagaoka-ct.ac.jp.

10.1021/jp022227h CCC: $25.00
Published on Web 02/04/2003

TABLE 1: Chemical Composition of Reactant Mixtures, Crystallization Temperatures, and Unit Cell Compositions of Products[a]

sample no.	Si/Al	NaF	NaOH	$AlCl_3$	SiO_2	H_2O	temp/K	unit cell composition
1	5.19	2.4	3	1	4.0	120	438	$Na_{7.45}(AlO_2)_{7.76}(SiO_2)_{40.24}$
2	5.71	2.7	3	1	4.5	135	438	$Na_{7.04}(AlO_2)_{7.15}(SiO_2)_{40.85}$
3	6.37	3.3	3	1	5.5	165	453	$Na_{6.37}(AlO_2)_{6.51}(SiO_2)_{41.49}$
4	7.65	8.3	3	1	5.5	165	438	$Na_{5.33}(AlO_2)_{5.55}(SiO_2)_{42.45}$
5	8.11	7.5	3	1	7.5	225	438	$Na_{5.14}(AlO_2)_{5.27}(SiO_2)_{42.73}$
6	9.00	8.0	3	1	8.0	240	438	$Na_{4.67}(AlO_2)_{4.80}(SiO_2)_{43.20}$

[a] Crystallization time was 72 h for each run.

TABLE 2: Crystallographic Data for Typical MS-F Samples

	sample 1	sample 4	sample 6
lattice constant *a* /nm	1.8112(5)	1.8108(3)	1.8110(2)
b/nm	2.0475(5)	2.0428(3)	2.0404(2)
c/nm	0.7523(2)	0.7504(1)	0.7494(1)
Cell volume/nm^3	2.790	2.776	2.769
R_{wp}/%	9.19	9.76	8.73
R_I/%	3.26	3.63	2.79
R_F/%	3.07	2.66	2.46
R_e/%	6.44	6.34	6.52
S factor (R_{wp}/R_e)	1.43	1.42	1.34
number of peaks	1455	1451	1449

2.2 Characterization. *Physicochemical Characterization.* X-ray diffraction (XRD) patterns of prepared crystals were collected by a powder X-ray diffractometer (Material Analysis and Characterization Inc., MXP-3) with graphite monochromatized Cu Kα radiation ($\lambda = 0.15418$ nm) at 40 kV and 30 mA. The Chemical composition of each product was determined by elemental Na, Al, and Si analysis using an inductively coupled plasma analyzer (Perkin-Elmer Optima-3000). Concentration of fluoride ion on surface and that at the 440 nm depth from the sample surface were analyzed by X-ray photoelectron spectroscopy (Shimadzu ESCA-3400). Field emission scanning electron microscopy (FE-SEM, HITACHI S-4500) was used to characterize the size and morphology of the obtained crystals. Electron diffraction and high-resolution transmission electron microscopy (JEOL JEM4000EX) were used to determine the crystallographic orientation. Solid-state MAS NMR spectra were measured by a Varian Unity-400 plus spectrometer. The ^{29}Si and ^{27}Al spectra were recorded at room temperature at 79.459 and 104.214 MHz, respectively, with a spinning rate of 6 kHz, by a single pulse technique. The pulse width was 5.5 μs ($\pi/2$ pulse) for ^{29}Si, and 2 μs for ^{27}Al. Chemical shifts are recorded relative to TMS for ^{29}Si and $[Al(H_2O)_6]^{3+}$ for ^{27}Al.

Adsorption isotherms of benzene on MS-F samples were measured gravimetrically at 298 K by use of a laboratory-made apparatus equipped with a quartz spring balance. Each sample was heated in vacuo (1 mPa) at 773 K for 5 h prior to the adsorption measurement.

The thermal stabilities of the products were investigated as follows. Hydrated samples were heated at a given temperature (927−1127 K) for 1 h in air. After cooling, they were rehydrated, and their XRD patterns were measured. The change in crystallinity of a sample on heating was elucidated. The crystallinity was determined by the integrated intensities of reflections (*I*) of eleven peaks indexed as 110, 020, 200, 111, 130, 310, 400, 150, 202, 350, and 511 as: crystallinity = $100 \times I_n/I_{298}$ (%) where I_n stands for *I* of the sample heated at *n* K.

Structure Refinement by Rietveld Method. Typical samples, those numbered 1, 4, and 6, were analyzed by the Rietveld method. Diffractograms of MS-F were collected by a Rigaku RINT-2500V. Copper Kα radiation monochromatized by a graphite crystal was used with tube voltage 30 kV and tube current 200 mA. Other measurement conditions were as follows: measured angle 18 to 95 × 2θ, stepping angle 0.05°, accumulation time 1 s, scattering slit 0.5°, divergence slit 0.5°, and receiving slit 0.15 mm. The RIETAN computer program for Rietveld analysis by Izumi[17] was used.

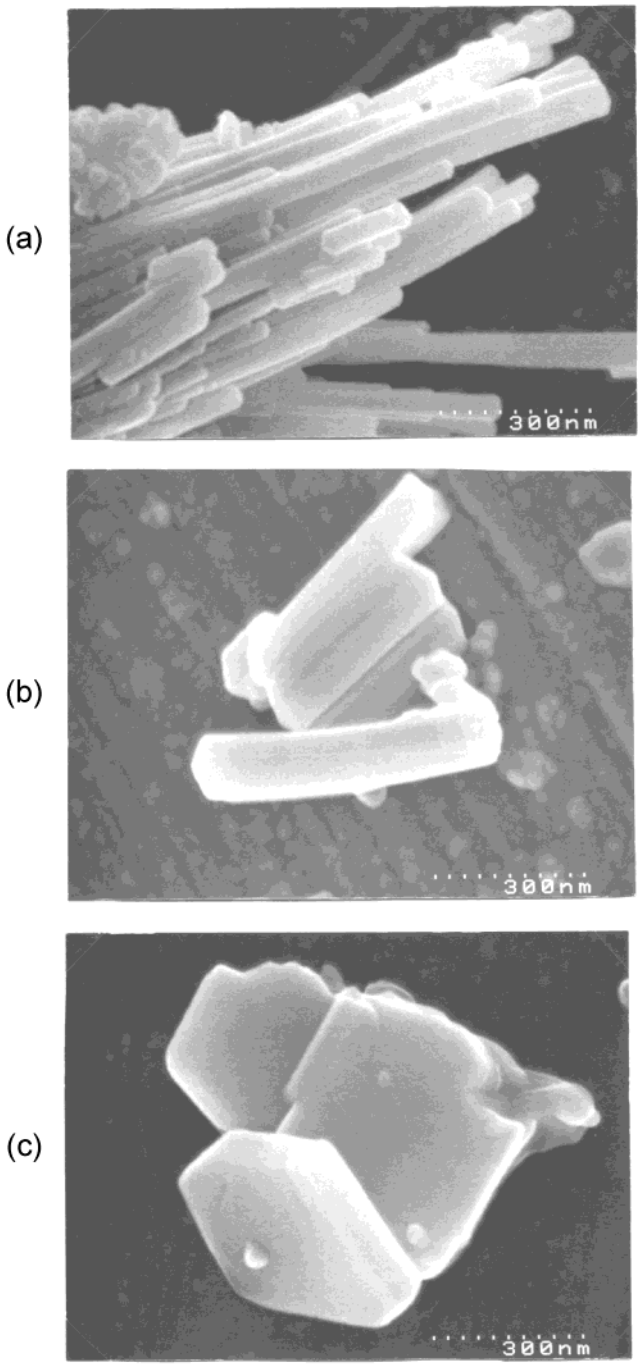

Figure 1. SEM images of synthesized MS-F crystals with different Si/Al ratios. (a) Sample 1; (b) sample 4; (c) sample 6.

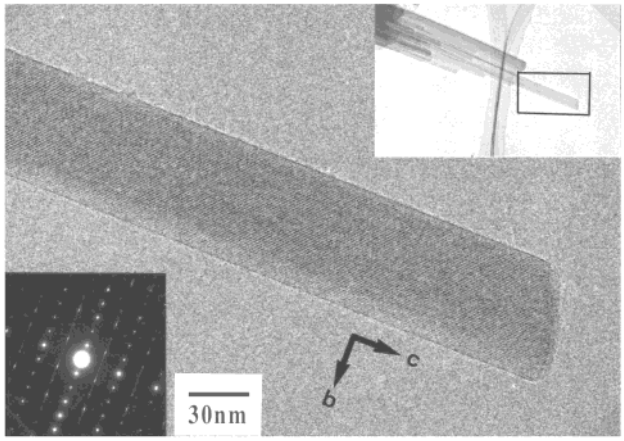

Figure 2. High-resolution electron micrograph of sample 1. Inset shows the corresponding electron diffraction pattern.

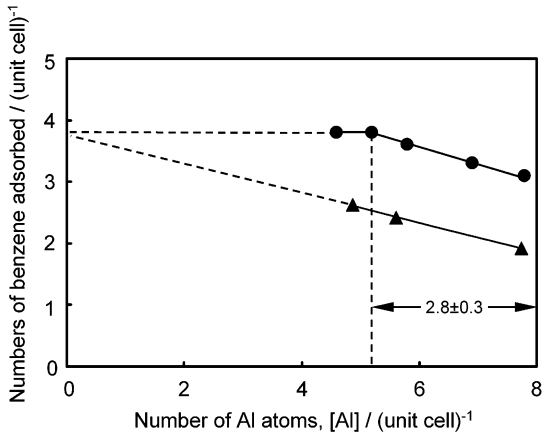

Figure 3. Dependence of adsorption of benzene molecules on the Al contents in MS-F (▲) and MS-C (●).

The structure of MS-F was refined on the basis of the initial atomic coordinates obtained by Meier[18] and Shiokawa et al.[19] with space group *Cmcm*. No constraint on the T−O bond length. The peak profile was assumed to be a pseudo-Voigt function. The zero-point shift, background parameters, peak profile factors, and lattice constants were initially refined. Then, atomic coordinates and isotropic thermal factors of the individual sites were refined. Occupancy factors of the framework sites were fixed at unity, and those of the extraframework cation and water molecules were also fixed because of the problem of divergence. The weighted pattern *R* indices (R_{wp}) and *S* factors defined by $S = R_{wp}/R_e$ (R_e: expected *R* index) were below 10% and ca. 1.4, respectively, as listed in Table 2, and no additional electron density was found by difference Fourier synthesis. The refinements appear to have been successful.

3. Results

3.1. Characteristics of MS-F Crystals. *Structural Characteristics.* MS-F with Si/Al ratios of 5.19−9.00 were successfully prepared in fluoride-containing reactant mixtures as shown in Table 1. The cocrystallization of analcime and contamination with MFI were observed at Si/Al ratios below 5.19 and above 9.00, respectively. The final pH of the mixtures after crystallization was ca. 10.5, which was lower than that for the MS-C formation (>12). No fluoride ion was detected by XPS on the surface and at a 440 nm depth, in any MS-F crystals after washing with a sufficient amount of hot water. MS-F crystals with the low Si/Al ratio of 5.19 consisted of agglomerates of needle type crystallites, and the crystal habit gradually varied to be platy with increasing Si/Al ratio up to 9.00, as shown in Figure 1. As shown in Figure 2, the *c* axis of the MS-F was parallel to the long side of a needle crystallite. The *c* axis of a platy crystallite with a high Si/Al ratio was parallel to the flat planes, in contrast to MS-C where the *c* axis was perpendicular to a platy crystallites.[20] These results suggest that the processes of nucleation and crystal growth in MS-F were different from those in MS-C. In zeolite formation in the presence of fluoride ion, active fluoride species such as fluorosilicates and fluoroaluminates are formed and those affect the crystallization processes.[21,22] In the present case, such species would be also formed in the reaction systems, resulting in the formation of different crystal habits from MS-C.

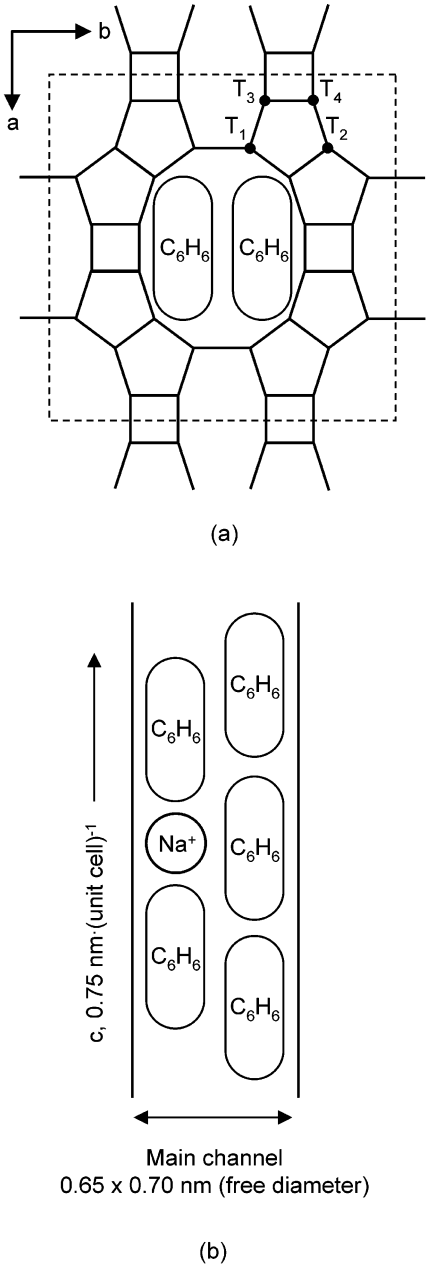

Figure 4. Configuration of benzene molecules and Na^+ ions in the main channel.

Benzene Adsorptivity and Cation Sites. The adsorption isotherm of benzene on sodium form MS-F was of type I in the IUPAC classification, regardless of Si/Al ratios; the adsorption capacity of benzene was determined by a Langmuir plot.

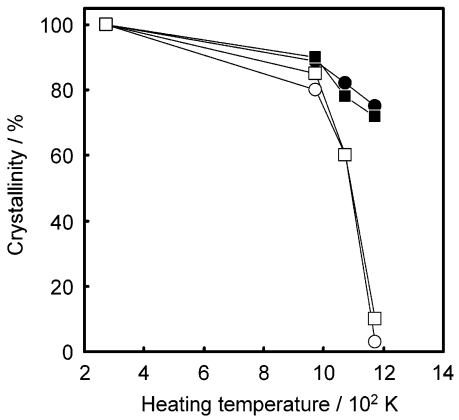

Figure 5. Thermal stability of synthesized MOR-type zeolites. ●, MS-F(Si/Al = 5.5); ■, MS-F(Si/Al = 8.2); ○, MS-C(Si/Al = 6.0); □, MS-C(Si/Al = 8.7).

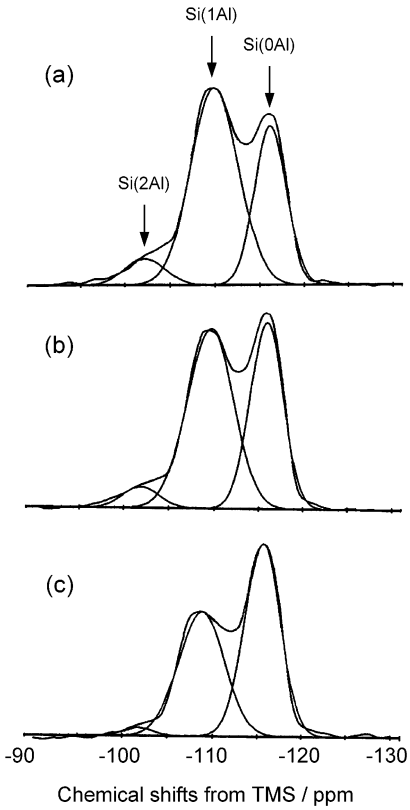

Figure 6. ^{29}Si MAS NMR spectra of MS-F with different Al content deconvoluted by three peaks. (a) Sample 1; (b) sample 3; (c) sample 6.

The experimental error for the adsorption capacity was less than ±0.1 molecules per unit cell. The adsorption capacity on the MS-F linearly decreased with increasing the number of Al atoms in a unit cell (u.c.), [Al], as shown in Figure 3. The adsorption capacity was significantly lower than that on MS-C of the same [Al]. Regarding MS-C, Itabashi reported that sodium ions in the main channels hinder diffusion of benzene molecules into the channels and exclude benzene molecules, thereby, the number of adsorbed benzene molecules of MS-C depends on [Al] in the range of [Al] = 5.2−8.[23] From the relationship between [Al] and the benzene uptake, the "exclusion length" for the benzene molecule by a sodium ion in the main channel could be estimated as 0.201 nm.[23] The exclusion length for the MS-F was obtained as 0.18 nm from Figure 3. These exclusion lengths reasonably coincided with the ionic diameter of a sodium ion 0.190 nm, which indicates that benzene molecules are adsorbed in the main channel of MS-F in the same manner as in MS-C.[5]

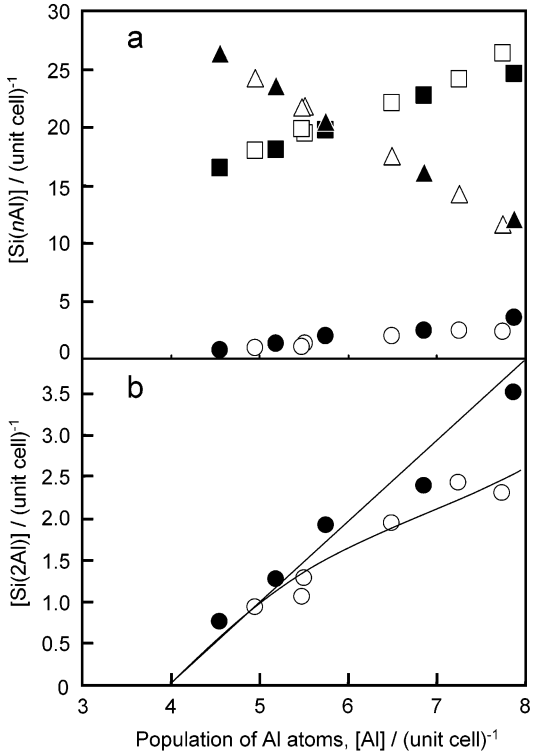

Figure 7. Dependence of the population of Si(nAl) on Al content (a) and magnified figure for the Si(2Al) changes. Circles, Si(2Al); squares, Si(0Al); triangles, Si(0Al). Open, MS-F; solid, MS-C.

TABLE 3: Populations of [Si(*n*Al)] Obtained from ^{29}Si MAS NMR Spectra of F/MOR

sample no.	Al content by NMR	Al content by chemical analysis	population of [Si(nAl)] [Si(2Al)]	[Si(lAl)]	[Si(0Al)]
1	7.7_4	7.76	2.3_0	26.3_5	11.6_1
2	7.2_5	7.15	2.4_3	24.1_4	14.1_9
3	6.4_9	6.51	1.9_5	22.0_8	17.4_8
4	5.5_1	5.55	1.2_8	19.4_8	21.7_3
5	5.4_8	5.27	1.0_6	19.7_9	21.6_7
6	4.9_5	4.80	0.9_4	17.9_2	24.1_8

As already reported in a previous paper,[5] a portion of sodium ions (2.8 per unit cell) of the eight extraframework sodium ions are located at sites facing the main channels in the MS-C with [Al] = 8, and they disturb the adsorption of benzene molecules, as schematically shown in Figure 4, parts a and b, because the number of adsorbed benzene molecule depends on the number of sodium ions, [Na], at 5.2 < [Na] < 8. These sodium ions in the main channel are preferentially removed by the displacement of Al by Si atoms until [Al] = 5.2, and then the residual 5.2 ions are substituted until [Al] = 4.6. When [Al] is less than 5.2, the adsorbed amount of benzene molecules is 3.8 molecules per unit cell regardless of the number of sodium ions. This phenomenon suggests that all sodium cations of MS-C with [Al] < 5.2 are in the side pockets.

On the other hand, in the case of MS-F, the adsorption capacity of benzene depends linearly upon [Al] over the whole concentration range at 4.80 < [Al] < 7.76, and the extrapolation intercepts the ordinate at 3.8, which means that the adsorption capacity of benzene in siliceous MS-F is equal to that obtained in the MS-C system. Such a different adsorption behavior

TABLE 4: Fractional Coordinates of Framework Atoms[a]

		sample 1	sample 4	sample 6
T_1	*x*	0.192(2)	0.195(1)	0.194(1)
	y	0.422(1)	0.426(1)	0.426(1)
	z	0.533(4)	0.535(2)	0.545(2)
	B	3.3(4)	2.2(2)	2.9(2)
T_2	*x*	0.199(1)	0.195(1)	0.195(1)
	y	0.186(1)	0.189(1)	0.189(1)
	z	0.523(3)	0.539(2)	0.543(1)
	B	3.3	2.2	2.9
T_3	*x*	0.090(2)	0.0836(11)	0.0869(9)
	y	0.381(2)	0.3818(12)	0.3829(9)
	z	1/4	1/4	1/4
	B	3.3	2.2	2.9
T_4	*x*	0.090(2)	0.0934(12)	0.0864(9)
	y	0.224(2)	0.2249(11)	0.2249(8)
	z	1/4	1/4	1/4
	B	3.3	2.2	2.9
O_1	*x*	0.129(3)	0.118(2)	0.122(1)
	y	0.418(2)	0.410(1)	0.410(1)
	z	0.429(5)	0.439(3)	0.440(3)
	B	4.6(4)	2.7(3)	3.9(2)
O_2	*x*	0.124(2)	0.126(1)	0.123(1)
	y	0.202(2)	0.199(2)	0.194(2)
	z	0.454(5)	0.441(4)	0.434(2)
	B	4.6	2.7	3.9
O_3	*x*	0.272(3)	0.271(2)	0.262(1)
	y	0.379(2)	0.371(2)	0.372(1)
	z	0.512(5)	0.509(4)	0.509(2)
	B	4.6	2.7	3.9
O_4	*x*	0.080(2)	0.085(2)	0.090(1)
	y	0.303(4)	0.308(3)	0.313(1)
	z	1/4	1/4	1/4
	B	4.6	2.7	3.9
O_5	*x*	0.177(3)	0.178(2)	0.180(2)
	y	0.205(4)	0.187(3)	0.198(2)
	z	3/4	3/4	3/4
	B	4.6	2.7	3.9
O_6	*x*	0.160(4)	0.150(2)	0.162(2)
	y	0.422(2)	0.420(2)	0.424(1)
	z	3/4	3/4	3/4
	B	4.6	2.7	3.9
O_7	*x*	0.228(3)	0.235(2)	0.222(2)
	y	1/2	1/2	1/2
	z	1/2	1/2	1/2
	B	4.6	2.7	3.9
O_8	*x*	1/4	1/4	1/4
	y	1/4	1/4	1/4
	z	1/2	1/2	1/2
	B	4.6	2.7	3.9
O_9	*x*	0	0	0
	y	0.398(4)	0.407(3)	0.401(2)
	z	1/4	1/4	1/4
	B	4.6	2.7	3.9
O_{10}	*x*	0	0	0
	y	0.190(5)	0.203(4)	0.204(3)
	z	1/4	1/4	1/4
	B	4.6	2.7	3.9

[a] The occupation factor was fixed at unity for each atom.

indicates that the location of sodium ions in the main channel of MS-F is different from that of MS-C even at the same [Al]. Judging from the relationship between the adsorption capacity and [Al], the number of sodium ions located at sites in main channels of MS-F can be eight at [Al] = 8, and sodium ions would be removed one by one through a substitution of Al by Si until [Al] = 4.87. This phenomenon strongly suggests that all Al atoms are located on the sites facing the main channel.

In the case of MS-C, a 3c superlattice has previously been considered in developing an ordered model distribution of aluminum sites since the number of sodium ion in the main channel is 2.8.[5] On the other hand, the number of sodium ions in the main channel of MS-F was eight, which means that it is not necessary to assume any superlattice of MS-F in a determination of Al site distribution. Consequently, the conventional unit cell with 48T atoms is used in building distribution models for MS-F.

TABLE 5: Fractional Coordinates of Extraframework Atoms[a]

		sample 1	sample 4	sample 6
W_1	*x*	1/2	1/2	1/2
	y	0.114(13)	0.113(10)	0.114(13)
	z	1/4	1/4	1/4
	B	35(3)	33(2)	35(3)
W_2	*x*	0.423(7)	0.424(5)	0.423(7)
	y	0.211(7)	0.229(5)	0.211(7)
	z	1/4	1/4	1/4
	B	35	33	35
W_3	*x*	1/2	1/2	1/2
	y	0.290(18)	0.295(11)	0.290(20)
	z	1/4	1/4	1/4
	B	35	33	35
W_4	*x*	1/2	1/2	1/2
	y	0.374(5)	0.399(5)	0.374(5)
	z	0.502(21)	0.483(12)	0.502(21)
	B	35	33	35
W_5	*x*	0.390(7)	0.386(6)	0.390(7)
	y	0.495(6)	0.493(4)	0.495(7)
	z	1/4	1/4	1/4
	B	35	33	35
Na_1	*x*	1/2	1/2	1/2
	y	0	0	0
	z	1/2	1/2	1/2
	B	33(5)	31(5)	33(5)
Na_2	*x*	0	0	0
	y	0.434(6)	0.434(5)	0.434(6)
	z	3/4	3/4	3/4
	B	33	31	33

[a] The occupation factor was fixed at unity for each atom.

TABLE 6: Mean Bond Length between T and O Sites

	mean bond length/nm		
	sample 1	sample 4	sample 6
T_1−O	0.160(17)	0.173(10)	0.163(4)
T_2−O	0.159(15)	0.153(10)	0.157(5)
T_3−O	0.167(7)	0.160(7)	0.159(10)
T_4−O	0.170(5)	0.169(5)	0.168(7)

Thermal Stability. The thermal stabilities of MS-F and MS-C were elucidated by the changes in the crystallinity with heating as shown in Figure 5. The crystallinity of MS-C abruptly decreased by heating above 1000 K, which indicates the collapse of the framework structure of MS-C. On the other hand, MS-F maintained more than 70% of its crystallinity to 1150 K regardless of Si/Al ratios. Because the framework topologies as well as natures of extraframework cations and zeolitic water are substantially identical for MS-F and MS-C, the difference in the thermal stability is apparently attributable to the difference in the Al distribution between MS-F and MS-C.

3.2. ^{29}Si and ^{27}Al MAS NMR of MS-F. As shown in Figure 6, ^{29}Si MAS NMR spectra of MS-F with various Si/Al ratios exhibited signals attributable to Si(2Al), Si(1Al), and Si(0Al) environments at −102, −108, and −116 ppm, respectively. Each signal was deconvoluted by curve fitting by applying a Gaussian line shape. Populations of Al atoms in the different environments, [Si(*n*Al)], were determined as summarized in Table 3. The Al contents of the samples calculated from NMR spectra agreed well with those determined by chemical analysis.

The changes in [Si(*n*Al)] of MS-F were shown in Figure 7a along with those of MS-C.[5] The number of all Si(*n*Al) species varied near linearly in the range of [Al] from 4 to 8 for both

TABLE 7: Connectivity Matrix of T Sites in a Single Unit Cell of MOR-Type Zeolite[a]

	$T_{1,j}$																$T_{2,j}$																$T_{3,k}$								$T_{4,l}$							
	1	2	3	4	5	6	7	8	9	10	11	12	13	14	15	16	1	2	3	4	5	6	7	8	9	10	11	12	13	14	15	16	1	2	3	4	5	6	7	8	1	2	3	4	5	6	7	8
$T_{1,1}$				1		1	*										*								*				1				1				*				*					*		
$T_{1,2}$			1		1			*										*								*				1				1	*					*				*		
$T_{1,3}$		1		*			1												*								*				1				*	1					*				*	
$T_{1,4}$	1				*	1														*								*				1	*			1				*				*		
$T_{1,5}$		1	*				1														*			1					*				1	*							*				*	
$T_{1,6}$	1			*		1																*			1				*				1			*								*		
$T_{1,7}$	*			1		1																	*			1				*			*			1					*				*	
$T_{1,8}$		*	1		1																			*			1				*			*	1					*				*	
$T_{1,9}$												1		1	*			*			1				*				1					*				1			*					*	
$T_{1,10}$											1		1			*	*					1				*												1	*		*					*	
$T_{1,11}$										1			*			1				*			1				*												1		*					*	
$T_{1,12}$									1					*	1					*				1				*												1		*					*	
$T_{1,13}$										1	*					1	1				*								*											1	*					*	
$T_{1,14}$									1			*			1			1			*									*											1		*					*	
$T_{1,15}$									*			1		1					1				*								*										1		*					*	
$T_{1,16}$										*	1		1							1			*								*											1		*					*	
$T_{2,1}$	*									*			1									1				*			1				*								1					*		
$T_{2,2}$		*								*				1							1				*				*					*								1				*		
$T_{2,3}$			*								*				1							1				*				*					*								1				*	
$T_{2,4}$				*								*				1							1				*				*					*								1				*
$T_{2,5}$					*				1					*				1						1				*				*								1				*		
$T_{2,6}$						*				1			*				1							1				*				*								1				*		
$T_{2,7}$							*				1					*			1							1				*					*								1				*
$T_{2,8}$								*				1			*			1								1				*					*								1				*
$T_{2,9}$		*			1				*									*				1							1					*								*					
$T_{2,10}$	*					1				*							*						1							1				*								*					
$T_{2,11}$				*			1				*									*				1							1				*								*				
$T_{2,12}$			*					1				*							*						1							1				*								*				1
$T_{2,13}$	1				*								*				1				*								*								*								1			
$T_{2,14}$		1		*										*				1			*								*					*								1				
$T_{2,15}$			1					*							*				1				*								*					*								1			1
$T_{2,16}$				1			*									*				1			*								1				*								1				
$T_{3,1}$	1			*		1	*										*				*				*				*					1								1					
$T_{3,2}$		1	*		1			*										*				*				*				*				1								1				
$T_{3,3}$		*	1		*			1											*				*				*				*			1								1				
$T_{3,4}$	*			1		*	1													*				*				*				*		1								1				
$T_{3,5}$								1				*			1	*		*			*				*				*								1									
$T_{3,6}$									1	*		1				*	*			*			*				*				*								1							
$T_{3,7}$									*	1		*				1			*			*				*				*								1							
$T_{3,8}$								*			1			*	1			*				*				*				*								1							1
$T_{4,1}$	*					*				*				*			1				1				*				*				1									1				
$T_{4,2}$		*			*				*				*					1		1				*				*				1									1				
$T_{4,3}$			*				*				*				*				1			1				*				*				1								1			
$T_{4,4}$				*				*				*				*				1			1				*				*				1								1		
$T_{4,5}$		*			*				*				*					*			*				1				1													1		
$T_{4,6}$	*					*				*				*			*				*				1				1													1	
$T_{4,7}$				*			*				*				*				*			*				1				1													1	
$T_{4,8}$			*					*				*				*				*				*				1				1													1

[a] Keys: 1, direct-neighbor each other; *, T sites are located in the same 5-ring.

MS-C[5] and MS-F; however, the changes in each [Si(*n*Al)] for MS-F were different from that for MS-C at the same [Al]. Actually, as shown in Figure 7b, careful observation of the changes in [Si(2Al)] for MS-F and MS-C revealed that the [Si-(2Al)] in MS-F varied nonlinearly with [Al] and was extrapolated to between 2 and 3 at [Al] = 8 although the number in MS-C changed linearly with [Al] and was extrapolated to 4 at [Al] = 8. These results also imply that the aluminum distribution in MS-F is different from that in MS-C. ^{27}Al MAS NMR spectra of all MS-F samples showed only one single peak attributable to the tetrahedral Al atom, which shows that all aluminum atoms in MS-F are incorporated in the framework.

3.3. Rietveld Analysis of MS-F. Rietveld analysis was applied for the MS-F samples, Nos. 1, 4, and 6, in Table 1, and are obtained fractional coordinates of framework sites and extraframework atoms and water molecules are summarized in Tables 4 and 5, respectively.

Bond lengths between the T site and oxygen atom were listed in Table 6. According to Jones, the bond length reflects the occupancy of the Al atom in a given T site; that is, the longer the bond lengths, the more Al atoms that occupy the site.[24] He also reported the relationship between the T−O bond length and the Al occupation at the T site, and suggested that the Al occupation at T_1, T_2, and T_4 sites can be regarded as constant.[24] Consequently, in the present case, it appears that the Al occupancy at T_1 and T_4 sites is higher than those at T_2 and T_3 sites, and that at the T_3 site, it decreases with a decrease of the Al content. The change in T_3−O length in Table 6 suggests that small amount of Al atoms are located at the T_3 sites in sample 1 and no Al atoms occupy the site in samples 4 and 6. The site occupied by Al atoms should be determined by considering not only these XRD data but also the other data such as NMR results, and consistent results should be obtained.

3.4. Determination of the Distribution of Al Atoms in the Framework of MS-F. A modification for the distribution of Al atoms in the framework of MS-F was determined by the results of ^{29}Si MAS NMR spectra analysis applying the CCM method under consideration of the results of benzene adsorption, thermal stability, and structural information obtained from Rietveld analysis.

In principle, the connectivity matrix describes connectivity relations between two T sites. The matrix was prepared without considering any symmetry of the framework but retaining the generality of the zeolite structure. Thus, the connectivity matrix

TABLE 8: (a) Configuration Matrix of Ordered Distribution of Al Atoms with Space Group *Pc* and (b) Configuration Matrix of [Si(2Al)] = 3 Derived from That with Space Group *Pc*[a]

site	$T_{1,i}$																$T_{2,j}$																$T_{3,k}$								$T_{4,l}$							
	1	2	3	4	5	6	7	8	9	10	11	12	13	14	15	16	1	2	3	4	5	6	7	8	9	10	11	12	13	14	15	16	1	2	3	4	5	6	7	8	1	2	3	4	5	6	7	8
$T_{1,1}$	\			1		1	*										*									*			1				1			*						*				*			
$T_{1,14}$									1			*		\	1			1			*								*							1			*			*						
$T_{2,6}$						*				1			*				1					\			1				*				*				*				1				*		
$T_{2,9}$		*			1				*									*			1		\						1					*			*					*			1		
$T_{4,3}$			*					*				*			*				1				1				*			*					1							1	\				
$T_{4,4}$				*			*				*					*				1			1				*				*				1								1	\			
$T_{4,7}$				*			*				*					*				*			*				1				1													1	\		
$T_{4,8}$			*					*				*			*				*				*					1			1														1	\	
sum	\	*	*	1	1	1	*	*	1	1	*	*	*	\	1	*	1	1	1	1	1	\	1	1	\	1	1	1	1	1	1	1	1	*	1	1	1	*	1	1	2	1	\	\	2	1	\	\

(b) Configuration matrix of [Si(2Al)]=3 derived from that with space group Pc

site	$T_{1,i}$																$T_{2,j}$																$T_{3,k}$								$T_{4,l}$							
	1	2	3	4	5	6	7	8	9	10	11	12	13	14	15	16	1	2	3	4	5	6	7	8	9	10	11	12	13	14	15	16	1	2	3	4	5	6	7	8	1	2	3	4	5	6	7	8
$T_{1,1}$	\			1		1	*										*									*			1				1			*						*				*			
$T_{1,14}$									1			*		\	1			1			*								*							1			*			*						
$T_{2,9}$		*			1				*									*			1		\						1					*			*					*			1		
$T_{3,6}$										1	*		1			*	*					*				*			*								\		1							1	
$T_{4,3}$		*						*				*			*				1				1				*			*					1							1	\				
$T_{4,4}$				*			*				*					*				1			1				*				*				1								1	\			
$T_{4,7}$				*			*				*					*				*			*				1				1													1	\		
$T_{4,8}$			*					*				*			*				*				*					1			1														1	\	
sum	\	*	*	1	1	1	*	*	1	1	*	*	1	\	1	*	*	1	1	1	1	*	1	1	\	*	1	1	1	1	1	1	1	*	1	1	1	\	1	2	1	1	\	\	2	2	\	\

[a] Keys in the sum: \, Al site; *, Si(0Al); 1, Si(1A1); 2, Si(2Al).

TABLE 9: Possible Configuration of Ordered Distributions of Al Atoms with [Si(2Al)] = 2 in the MS-F Framework with Any Symmetry Element, and the Derived Configurations, Which Satisfy Both of the Loewenstein's Rule and the 2 Al/5-Ring Avoidance Rule, with [Si(2Al)] = 3 by Movement of One of the Al Atoms from the Configuration in the Second Column

configuration	location of Al atoms	space group	location of Al atoms in the configuration with [Si(2Al)]=3
I	$T_{1,1}\,T_{1,2}\,T_{2,5}\,T_{2,6}\,T_{4,3}\,T_{4,4}\,\mathbf{T_{4,7}}\,\mathbf{T_{4,8}}$	$P2$	$T_{1,1}\,T_{1,2}\,T_{2,5}\,T_{3,6}\,T_{4,3}\,T_{4,4}\,T_{4,7}\,T_{4,8}$
I′	$T_{1,1}\,T_{1,2}\,T_{2,5}\,T_{2,6}\,\mathbf{T_{3,7}}\,\mathbf{T_{3,8}}\,T_{4,3}\,T_{4,4}$	$P\underline{2}$	none
II	$T_{1,1}\,T_{1,5}\,T_{2,2}\,T_{2,6}\,T_{4,3}\,T_{4,4}\,\mathbf{T_{4,7}}\,\mathbf{T_{4,8}}$	$P\bar{1}$	$T_{1,1}\,T_{1,5}\,T_{2,2}\,T_{3,6}\,T_{4,3}\,T_{4,4}\,T_{4,7}\,T_{4,8}$
II′	$T_{1,1}\,T_{1,5}\,T_{2,2}\,T_{2,6}\,\mathbf{T_{3,7}}\,\mathbf{T_{3,8}}\,T_{4,3}\,T_{4,4}$	$P\bar{1}$	none
III	$T_{1,1}\,T_{1,14}\,T_{2,6}\,T_{2,9}\,\mathbf{T_{4,3}}\,T_{4,4}\,\mathbf{T_{4,7}}\,T_{4,8}$	Pc	$T_{1,1}\,T_{1,14}\,T_{2,9}\,T_{3,6}\,T_{4,3}\,T_{4,4}\,T_{4,7}\,T_{4,8}$
III′	$T_{1,1}\,T_{1,14}\,T_{2,6}\,T_{2,9}\,\mathbf{T_{3,3}}\,\mathbf{T_{3,7}}\,T_{4,4}\,T_{4,8}$	Pc	none
IV	$T_{1,1}\,T_{1,16}\,T_{2,6}\,T_{2,11}\,\mathbf{T_{4,2}}\,\mathbf{T_{4,3}}\,T_{4,5}\,\mathbf{T_{4,8}}$	Pc	none
IV′	$T_{1,1}\,T_{1,16}\,T_{2,6}\,T_{2,11}\,\mathbf{T_{3,2}}\,\mathbf{T_{3,8}}\,T_{4,3}\,T_{4,5}$	Pc	none
IV″	$T_{1,1}\,T_{1,16}\,T_{2,6}\,T_{2,11}\,\mathbf{T_{3,3}}\,\mathbf{T_{3,5}}\,T_{4,2}\,T_{4,8}$	Pc	none

of 48 × 48 in regard to all combinations of T atoms for one unit cell was made as shown in Table 7. The symbol "1" in Table 7 stands for a direct-neighboring configuration of T sites. The symbol "*" means that each T site is located in the next-neighboring position in the same 5-ring. Considering the 2Al/5-ring avoidance rule,[5] T sites in the next-neighboring relationship, "*", cannot be simultaneously occupied by Al atoms. The distribution of 8 Al atoms on 48 T sites which satisfies the population of Si(*n*Al) determined by the NMR measurements was surveyed by using configuration matrixes as follows. Arbitrary eight rows corresponding to T sites occupied by Al atoms are chosen from the connectivity matrix, and a nonsquare, 8 × 48 matrix (called the configuration matrix) is constructed, and then the sum of the numbers in each column is written down in the ninth row as shown in Table 8a. When a column in the configuration matrix contains "\" and "*" simultaneously, the 2Al/5-ring avoidance rule has been violated. If the sum in the *i*th column is *n*, the Si atom on the *i*th site is in the state of [Si(*n*Al)]. Using this procedure, we can estimate the population of Si(*n*Al) for a given configuration directly and then compare with the observed ones by NMR spectra to check the validity of the configuration.

Now, suppose there is a random distribution of Al atoms on T sites in MOR-type framework subject only to Loewenstein's rule. In this case, all of the configurations that satisfy the Loewenstein's rule should exist in the framework of the zeolite. In the mordenite framework assuming the crystallographic unit cell repeat, the number of possible configurations is 19 656 828. If Al atoms are randomly distributed, the average populations of Si(*n*Al)s in MS-F with [Al] = 8 are [Si(0Al)] = 15.15, [Si(1Al)] = 18.25, [Si(2Al)] = 6.03, and [Si(3Al)] = 0.56. The calculated populations were quite different from the ones observed in sample 1 with [Al] = 7.74 as listed in Table 3. Therefore, the aluminum atoms would be regularly distributed in the framework.

From the CCM method, we can know the maximum number of Al atoms in the framework. When both the 2Al/5-ring avoidance rule and Loewenstein's rule are satisfied, the maximum number of Al atoms is 8. However, considering only Loewenstein's rule, the maximum number of Al atoms became 16. The maximum number obtained by synthesis was [Al] = 7.74 for MS-F (Table 3), which is comparable to the estimated number considering both the 2Al/5-ring avoidance rule and Loewenstein's rule. This means that it is reasonable to consider the 2Al/5-ring avoidance rule in determining the Al distribution in the framework, in addition to Loewenstein's rule.

No Si(3Al) was detected in MS-F by ^{29}Si NMR measurements regardless of the Si/Al ratio (Figure 6), and the extrapolated value of [Si(2Al)] at [Al] = 8 in MS-F was between two and three as already shown in Figure 7. Therefore, Al-rich MS-F would contain two configurations of the ordered distribution of Al atom with [Si(2Al)] = 2 and 3. The configuration with [Si(2Al)] = 3 would be obtained from the partial displacement of Al atom in the ordered distribution with [Si(2Al)] = 2. Even in this case, the 2Al/5-ring avoidance rule should be satisfied to retain thermal stability of MS-F.

TABLE 10: Population Changes by Substitution of Al by Si Atoms and by Misplacement of Al Atoms[a]

	population changes of [Si(*n*Al)]			
	Δ[Si(2Al)]	Δ[Si(1Al)]	Δ[Si(0Al)]	Δ[Al]
substitution of Al by Si atoms at				
(A) $T_{2,6}$, $T_{2,9}$, $T_{4,3}$ or $T_{4,7}$ site	−1	−2	+4	−1
(B) $T_{1,1}$, $T_{1,14}$, $T_{4,4}$ or $T_{4,8}$ site	0	−4	+5	−1
misplacement of Al atom				
(C) $T_{2,6}$ to $T_{3,6}$ site	+1	−2	+1	0

[a] (A) represents the substitution of Al by Si atoms at the sites of Al−O−Si−O−Al, (B) shows the substitution of Al by Si atoms at the sites of isolated Al atoms, and (C) shows the change from the configuration with [Si(2Al)] = 2 to that of 3 under the restriction of the 2Al/5-ring avoidance rule.

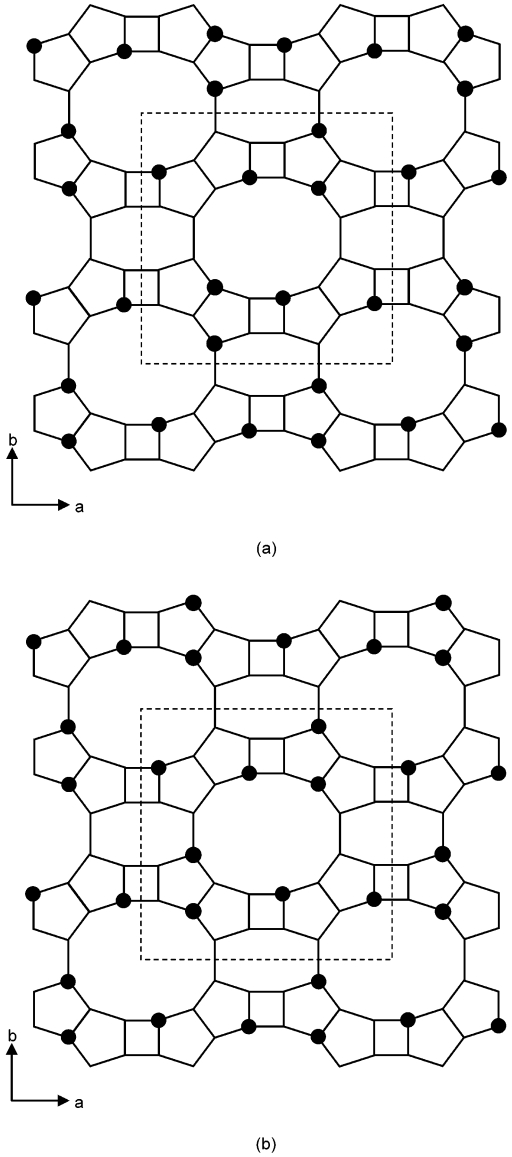

Figure 8. Projection to the *ab* plane of candidates of the ordered distribution of Al atoms in mordenite framework with [Si(2Al)] = 2 and with any symmetry element in the distribution. a and b correspond to the configurations I and II, and III, respectively. The difference between I and II in (a) is the Al position. The locations of $T_{1,2}$ and $T_{2,5}$ in configuration I, and that of $T_{1,5}$ and $T_{2,2}$ in configuration II, are related to upper and lower side in the plane of the sheet, respectively.

All possible configurations of Al atoms for [Al] = 8 in 48 T sites were calculated under the restriction of the above two rules. The number of topologically independent configurations was 151. Of these, 35 configurations have [Si(2Al)] = 2. Because the crystal is expected to be more stable when the configuration of Al atom sites has higher symmetry, nine configurations

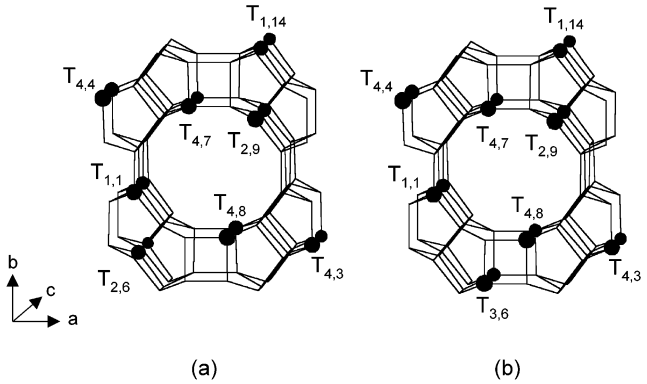

Figure 9. Three-dimensional structural model of mordenite and positions of 8 Al atoms. Configuration III with [Si(2Al)] = 2 for space group *Pc* (a), and that with [Si(2Al)] = 3 derived from space group *Pc* (b).

containing [Si(2Al)] = 2 with some symmetry listed in Table 9 remained as candidates from the 35 configurations. In these configurations, the configuration I′ can be regarded as a modified configuration of I, in which two Al atoms on $T_{4,7}$ and $T_{4,8}$ sites are moved to $T_{3,7}$ and $T_{3,8}$ sites. The relationships between II and II′, between III and III′, and between IV and IV′ or IV″ are similar to that between I and I′. Three kinds of the Al configurations, I, II, and III, projected in the *ab* plane are illustrated in Figure 8, parts a (for I and II) and b (for III). Further computational calculations were carried out using the CCM method for the change of [Si(2Al)] from 2 to 3 by the displacement of one Al atom to a next neighbor site without violating either Loewenstein's rule or the 2Al/5-ring avoidance rule. Such a change was possible when an Al atom at the $T_{2,6}$ site moved to the next neighbor $T_{3,6}$ site in the configurations I, II, and III, as summarized in Table 9. It should be noted that no Al atoms occupy T_3 sites in the configurations I, II, and III, that is, eight Al atoms per unit cell are located at the sites facing the main channel, T_1, T_2, and T_4. This is the marked difference from the distribution of Al atoms in MS-C. These results support that all sodium ions in MS-F are located in main channels, which agreed with the phenomena that all sodium cations disturb benzene adsorption. The difference in these configurations is the distribution of Al atoms in the wall of the main channel. Aluminum atoms are distributed in the same way in all main channels in the configuration III (Figure 8b), but those in the configurations I and II (Figure 8a) are not equivalent in the peripheries of the two main channels. Therefore, configuration III is considered the most plausible as a candidate of Al distribution in MS-F. Further analysis was attempted on the basis of configuration III.

The quantitative simulation is necessary to explain the observed ^{29}Si MAS NMR spectra of MS-F with different [Al] by (a) substitution of Al with Si in the decrease of [Al] and (b) misplacement of Al atoms from the ideal configuration. As

TABLE 11: Simulation of the Populations of Si(nAl) Based on the Ordered Distribution of Al Atoms in the Framework of MS-F

sample		ratio of the substitution A and B, and misplacement C in Table 10 A	B	C	[Al] /atoms (unit cell)$^{-1}$	population of [Si(*n*Al)] /atoms (unit cell)$^{-1}$ [Si(2Al)]	[Si(1Al)]	[Si(0Al)]
Ideal ordered distribution					8	2	28	10
sample 1	observed[a]				7.7_4	2.3_0	26.3_5	11.6_1
	calculated	0.0	0.26	0.31	7.7_4	2.3_1	26.3_4	11.6_1
	|(observed-calculated)|				0.0	0.0_1	0.0_1	0.0
sample 2	observed[a]				7.2_5	2.4_3	24.1_4	14.1_9
	calculated	0.05	0.7	0.48	7.2_5	2.4_3	24.1_4	14.1_8
	|(observed-calculated)|				0.0	0.0	0.0	0.0_1
sample 3	observed[a]				6.4_9	1.9_5	22.0_8	17.4_8
	calculated	0.05	1.46	0	6.4_9	1.9_5	22.0_6	17.5_0
	|(observed-calculated)|				0.0	0.0	0.0_2	0.0_2
sample 4	observed[a]				5.5_1	1.2_8	19.4_8	21.7_3
	calculated	0.72	1.77	0	5.5_1	1.2_8	19.4_8	21.7_3
	|(observed-calculated)|				0.0	0.0	0.0	0.0
sample 5	observed[a]				5.4_8	1.0_6	19.7_9	21.6_7
	calculated	0.94	1.58	0	5.4_8	1.0_6	19.8_0	21.6_6
	|(observed-calculated)|				0.0	0.0	0.0_1	0.0_1
sample 6	observed[a]				4.9_5	0.9_4	17.9_2	24.1_8
	calculated	1.06	1.99	0	4.9_5	0.9_4	17.9_2	24.1_9
	|(observed-calculated)|				0.0	0.0	0.0	0.0_1

[a] The values determined by ^{29}Si MAS NMR spectra.

TABLE 12: Occupation of Al Atoms Calculated from the Ordered Distribution of Al Atoms in the MS-F Framework and Successive Misplacement and Substitution of Al Atoms by the Change of Al Content

	T sites T_1	T_2	T_3	T_4
number of equivalent site /sites (unit cell)$^{-1}$	16	16	8	8
ideal ordered distribution /atoms (unit cell)$^{-1}$	2	2	0	4

sample no.	number of Al atoms/atoms(unit cell)$^{-1}$ (occupancy ratio) T_1	T_2	T_3	T_4
1	1.87 (0.12)	1.69 (0.11)	0.31 (0.04)	3.87 (0.48)
2	1.65 (0.10)	1.50 (0.09)	0.48 (0.06)	3.63 (0.45)
3	1.27 (0.08)	1.98 (0.12)	0 (0)	3.25 (0.41)
4	1.11 (0.07)	1.64 (0.10)	0 (0)	2.76 (0.35)
5	1.21 (0.08)	1.53 (0.10)	0 (0)	2.74 (0.34)
6	1.01 (0.06)	1.47 (0.10)	0 (0)	2.48 (0.31)

already mentioned, the framework of MS-F was thermally stable. This stability implies that the Al distribution in the framework obeys the 2Al/5-ring avoidance rule as in the case of heulandite and clinoptilolite.[7] The two kinds of substitution of Al by the Si atom in configuration III were considered to explain the ^{29}Si MAS NMR spectra and designated by (A) and (B) in Table 10. The population change of [Si(*n*Al)] depends on which site is substituted by the Si atoms. Now, we consider the ordering model of Al atoms in the framework as a basic model for the simulation. In configuration III, Al atoms are located at $T_{1,1}$, $T_{1,14}$, $T_{2,6}$, $T_{2,9}$, $T_{4,3}$, $T_{4,4}$, $T_{4,7}$, and $T_{4,8}$ sites as shown in Figure 9a. The configuration matrix with [Si(2Al)] = 3 by the misplacement of one Al atom from $T_{2.6}$ to $T_{3.6}$ and the corresponding Al atom sites in the framework are shown in Table 8b and Figure 9b, respectively. A population change of [Si(*n*Al)] also occurs with the misplacement as summarized in (C) in Table 10. The results of spectral simulations based on the above substitutions and misplacement in the MS-F samples are summarized in Table 11. The populations of Si(*n*Al)s in sample 1 in Table 11, for example, are calculated as $[\mathrm{Si}(n\mathrm{Al})]_{\text{ordered distribution}} + 0.0\Delta[\mathrm{Si}(n\mathrm{Al})]_A + 0.26\Delta[\mathrm{Si}(n\mathrm{Al})]_B + 0.31\Delta[\mathrm{Si}(n\mathrm{Al})]_C$. Namely, the population of Si(*n*Al) in sample 1 was shifted from that of the ordered distribution by the substitutions A and B, and the misplacement C at the ratio of 0, 0.26, and 0.31, respectively. The observed populations of [Si(*n*Al)] of all MS-F crystals used in this study are also in excellent agreement with the calculated values within 0.02. In the Al-rich samples, samples 1 and 2 in Table 11, a small number of Al atoms, 0.31−0.48 per unit cell, seem to occupy T_3 sites. In samples 3−6 with lower Al content, no Al atoms occupy the T_3 sites, and the substitution of Al atoms by Si atoms simply occurs because the ratio of the misplacement ("C" in Table 10) is zero. The partial occupation of Al atoms on T_3 sites in samples 1 and 2 may have taken place to alleviate the electrostatic repulsion between Al atoms in the wall of the main channel. Pure MS-F crystals with [Al] = 8 could not be prepared as a single phase, because of cocrystallization of analcime. In the case of MS-F with [Al] = 8, negative charges of Al sites should be localized on peripheries of the main channel; therefore, sodium ions should be also concentrated in the main channel. It would make the framework unstable.

4. Discussion

In configurations I and II, the same discussions can be made as those of configuration III, and the simulations of ^{29}Si MAS NMR spectra were equivalent to that for the configuration III. For this reason, the predominant configuration cannot be determined. The electrostatic field in the main channel of configuration III is more homogeneous than those of configurations I and II. Therefore, configuration III, with space group *Pc*, is the most suitable as the ideal distribution of Al atoms in the framework of MS-F with [Al] = 8.

In the cases of other zeolites, analcime,[25] epistilbite,[6] heulandite,[7] clinoptilolite[7] and dachiardite,[8] the calculated occupancies of Al atoms agree well with those estimated by XRD structural analysis by assuming that the configurations with higher symmetry are more stable than those with lower symmetry. To select the most suitable candidate of Al distribution in MS-F, we assumed that this assumption is again reasonable. Although the validity of this assumption is not yet clear, the present approach does throw light on the relationship between physicochemical characteristics and the Al configuration of zeolites.

The occupation of Al atoms in T sites can be calculated from an assumed ordered distribution, and successive misplacement and substitution of Al atoms are summarized in Table 11. Based upon those results, the occupancy of Al atoms at each site was calculated as shown in Table 12. The number of Al atom on T_1 sites is 2 of 16 in the ordered distribution, and those of the prepared samples decreased from 1.87 to 1.01 (from 0.12 to 0.06 as the occupancy ratio to the number of T_1 sites) on decreasing the total Al content from 7.76 to 4.80. Simultaneously, the occupancy ratio to the number of T_4 sites decreased from 0.48 to 0.31. As for T_2 sites, the occupation ratio was almost constant, 0.10, regardless of the total Al number. Although 0.31 and 0.48 of Al atoms were located on T_3 sites in samples 1 and 2 respectively, no Al atoms occupied at the sites in samples 3−6. These changes in Al location qualitatively agreed with that of the T−O length obtained from structural analysis as already mentioned.

5. Conclusions

MOR-type zeolite is synthesized in the gel containing fluoride ion (MS-F). The adsorptivity of benzene on MS-F was lower than that on MOR synthesized in the conventional gels without fluoride ion (MS-C). The difference in the adsorptivity is due to different cation distribution between MS-F and MS-C. The MS-F crystals are thermally more stable than the MS-C. The particle morphology of MS-F varies with the Si/Al ratio and is different from that of MS-C: MS-F with the low Si/Al ratio of 5.19 is of needle type crystallites, and the crystal habit gradually varied to be platy with increasing the Si/Al ratio up to 9.00. The *c* axis of the needlelike crystallite is parallel to the long side of a needle crystallite; however, that of the platy crystallite with a high Si/Al ratio is parallel to the flat plane in contrast to MS-C where the *c* axis was perpendicular to a platy crystallite. ^{29}Si MAS NMR reveals that MS-F contains a lower Si(2Al) population than MS-C. A different distribution of Al atoms between these zeolites can be deduced from these phenomena.

Models for ordered configurations of Al atoms in the framework of MS-F were determined by the CCM method using the 2Al/5-ring avoidance rule and the ^{29}Si MAS NMR spectral data. The Al atoms of MS-F are suggested to be ideally located only on the main channel sites, T_1, T_2, and T_4 sites with space group *Pc*, that is, $T_{1,1}$, $T_{1,14}$, $T_{2,6}$, $T_{2,9}$, $T_{4,3}$, $T_{4,4}$, $T_{4,7}$, and $T_{4,8}$. A small amount of misplacement of the Al atom from $T_{2,6}$ to $T_{3,6}$ is suggested in Al-rich MS-F. The unit cell of MS-F is the same as the conventional one composed of 48 T sites in contrast to MS-C which has a 3c superstructure with 36 T sites. The adsorption capacity of benzene for MS-F less than that of MS-C can be explained by different locations of sodium ions in the main channel which are caused by the different ordering of Al atoms between them. The calculated occupancies at the sites are in good agreement with those predicted by T−O bond length. The presence of fluoride ions in the synthesis of zeolites changes not only the crystal morphology but also the ordering of Al atoms in the framework. The 2Al/5-ring avoidance rule is a special case of the Dempsey rule, and the limitation of the rule is under investigation. So, it may not be able to be declared that another configuration is perfectly impossible. However, as mentioned above, it is considered that the possibility of existence of the configurations other than those used in the present investigation may be very low so far as the 2Al/5-ring avoidance rule is applied.

Acknowledgment. The authors are indebted to Professor Osamu Terasaki, Tohoku University, for his kind help on measurement and analysis of high-resolution transmission microscopy.

References and Notes

(1) Flanigen, E. M. In *Proceedings of the Fifth International Zeolite Conference*; Rees, L. V. C., Ed.; Heyden: London, 1980; p 760.
(2) Marcilly; C. *Stud. Surf. Sci. Catal.* **2001**, *135*, 37.
(3) Pavelic, K.; Subotic, B.; Colic, M. *Stud. Surf. Sci. Catal.* **2001**, *135*, 170.
(4) Baerlocher, Ch.; Meier, W. M.; Olson, D. H. *Atlas of Zeolites Framework Types*, 5th ed.; Elsevier: Amsterdam, 2001.
(5) Takaishi, T.; Kato, K.; Itabashi, K. *Zeolites* **1995**, *15*, 21.
(6) Kato, M.; Takahashi, K. In *Natural Zeolites for the Third Millennium*; Colella, C., Mumpton, F. A., Eds.; De Frede-Editore: Napoli, 2000; p 81.
(7) Kato, M.; Satokawa, S.; Itabashi, K. *Stud. Surf. Sci. Catal.* **1997**, *105*, 229.
(8) Kato, M.; Itabashi, K. *Stud. Surf. Sci. Catal.* **2001**, *135*, 240.
(9) Itabashi, K.; Fukushima, T.; Igawa, K. *Zeolites* **1986**, *6*, 30.
(10) Guth, J. L.; Kessler, H.; Caullet, P.; Hazm, J.; Merrouche, A.; Patarin, J. *Proceedings of the Ninth International Zeolite Conference*; von Ballmoos, R., Higgins, J. B., Treacy, M. M. J., Eds.; Butterworth-Heinemann: Boston, 1993: p 215.
(11) Caullet, P.; Guth, J. L.; Faust, A. C.; Joly, J. F.; Travers, C.; Razz, E. U.S. Patent 5,215,736, 1993.
(12) Joly, J. F.; Caullet, P.; Guth, J. L.; Faust, A. C.; Brunard, N.; Kolenda, F. U.S. Patent 4,853,203, 1994.
(13) Guth, J. L.; Faust, A. C.; Razz, F.; Lamblin, J. M. U.S. Patent 4,-853,203, 1989.
(14) Camblor, M. A.; Corma, A.; Valencia, S. *J. Mater. Chem.* **1998**, *8*, 213.
(15) Itabashi, K.; Hirano, S. *Japan Kokai Tokkyo Koho*, JP96−091827, 1996.
(16) Itabashi, K.; Kato, K.; Matsumoto, A.; K. Tsutsumi, K. *Extended Abstract of International Symposium on Zeolite and Microporous Crystals*; Sendai, Japan, 2000; p 16.
(17) Izumi, F. In *The Rietveld Method*; Young, R. A., Ed.; Oxford University Press: Oxford, 1993; Chapter 13.
(18) Meier, W. M. *Z. Kristallogr*. **1961**, *115*, 439.
(19) Shiokawa, K.; Ito, M.; Itabashi, K. *Zeolites* **1989**, *9*, 170.
(20) Terasaki, O.; Yamazaki, K.; Thomas, J. M.; Ohsuna, T.; Watanabe, D.; Sanders, J. V.; Barry, J. C. *J. Solid State Chem*. **1988**, *77*, 72.
(21) Guth, J. L.; Kessler, K.; Higel, J. M.; Lamblin, J. M.; Patarin, J.; Seive, A.; Chezeau, J. M.; Wey, R. In *Zeolite Synthesis*, ACS Symp. Ser. 398; Occelli, M. L., Robson, H. E., Eds.; American Chemical Society: Washington, DC, 1989; p 176.
(22) Gilson, J.-P. In *Zeolite Microporous Solids: Synthesis, Structure and Reactivity*; NATO ASI Series C.; 352; Derouane, E. G., Lemos, F., Naccache, C., Ribeiro, F. R., Eds.; Kluwer Academic Publishers: Dordrecht, The Netherlands, 1992; p 19.
(23) Itabashi, K.; Okada, T.; Igawa, K. *Stud. Surf. Sci. Catal.* **1986**, *28*, 369.
(24) Jones, J. B. *Acta Cryst*. **1968**, *24*, 355.
(25) Kato, M.; Hattori, H. *Phys. Chem. Miner*. **1998**, *25*, 556.